Annals of Anatomy 224 (2019) 124–132

Contents lists available at ScienceDirect

Annals of Anatomy

journal homepage: www.elsevier.com/locate/aanat

Amygdalin (Vitamin B17) pretreatment attenuates experimentally induced acute autoimmune hepatitis through reduction of CD4+ cell infiltration

Wael M Elsaed [a,b,*]

[a] Department of Anatomy, Taibah University, Almadinah Almounawrah, Saudi Arabia
[b] Anatomy and Embryology Department, Faculty of Medicine, Mansoura University, Egypt

ARTICLE INFO

Article history:
Received 20 February 2019
Received in revised form 18 April 2019
Accepted 24 April 2019

Keywords:
Autoimmune hepatitis
CD4+ cells
Amygdalin

ABSTRACT

Background: Autoimmune hepatitis (AIH) is an immune-mediated inflammation of the liver characterized by disorganized hepatic parenchyma and inflammatory cell infiltration. Although the increased incidence of AIH, the development of novel therapeutic strategies are impeded by the poor understanding of the accompanied detailed immunopathogenic changes. CD4+ T cells are key mediators of inflammatory cell infiltration in initial phases of liver injuries like AIH. The distribution of CD4+ cells and the histopathological changes accompanying Con A-induced AIH were investigated together with the postulated protective effect of Amygdalin (Amg.).

Materials and methods: 30 adult male mice were divided into three groups; control, AIH and AIH-Amg. groups. AIH was induced by a single intravenous injection of Concanavalin A (Con A) (15 mg/kg). The AIH-Amg. group received Amg. 5 mg/kg intraperitoneally once a week for three weeks. Blood samples were examined for ALT and AST. MDA, SOD, and GSH were determined in hepatic homogenates. Liver section stained with hematoxylin and eosin, Masson trichrome and CD4+ immune stain were examined by light and electron microscopy.

Results: AIH group showed a significant increase in levels of ALT, AST and MDA and a significant decline in SOD and GSH compared to the controls. The liver tissue showed distorted hepatic architecture with intercellular hemorrhage, necrosis, and inflammatory cell infiltration. The area percent of CD4+ immune staining was significantly increased. Electron microscopic examination showed massive cellular degenerative changes. Amg. pretreatment in AIH-Amg. group significantly reversed these changes.

Conclusion: AIH induced CD4+ cells infiltration in the liver with subsequent liver tissue damage. Amg. pretreatment inhibited CD4+ cell infiltration and protected the liver tissue. This finding suggests that Amg. could be a therapeutic agent in the management of AIH.

1. Introduction

Autoimmune hepatitis (AIH) is an immune-mediated inflammation of the liver characterized by disorganized hepatic parenchyma and inflammatory cell infiltration (Christen and Hintermann, 2016). The exact etiology of AIH is still unknown (Aizawa and Hokari, 2017), however, different pathogens as environmental factors, viruses and chemicals have been postulated (Czaja, 2011). AIH reported a progressive increased prevalence and incidence in all ages and ethnic groups (Gatselis et al., 2015). Yet, the management of AIH is still largely restricted to steroids and cytostatic drugs (Czaja, 2011). The poor understanding of the detailed immunopathogenic changes accompanying AIH hampers the development of novel therapeutic strategies (Burak et al., 2013).

A known experimental model of drug-induced AIH in mice is the use of Concanavalin A (Con A) (Mao et al., 2015). Con A-induced acute hepatitis matches the histopathological picture of AIH patients (Ye et al., 2018). Induced autoimmune hepatitis involves the release of inflammatory mediators and inflammatory cell infiltration. These pathologic changes can proceed with time to chronic liver disease (De Biasio et al., 2006). As in other body tissues, the orderly step that follows inflammation is tissue healing by fibrosis which is a beneficial reversible defense mechanism aiming to encapsulate the tissue injury (Ebrahimi et al., 2016). However, the ultimate progression to advanced hepatic fibrosis and/or cir-

* Corresponding author at: Department of Anatomy, Taibah University, Almadinah Almounawrah, Saudi Arabia.
E-mail address: wzaarina@taibahu.edu.sa

https://doi.org/10.1016/j.aanat.2019.04.006
0940-9602/

rhosis, which is an irreversible tissue response, disrupt the liver architecture and function (Friedman, 2008).

CD4+ cells are key mediators of inflammatory responses which play a crucial role in initial phases of liver injury, regeneration and graft rejection (Yamamoto et al., 2002). CD4+ cells were supposed to induce cytokine responses that control liver response to injury (Salgame et al., 1991). CD4+ cells were reported to direct the Con A-induced AIH through oxidative stress (Tiegs et al., 1992). Furthermore, the absence of CD4+ cells was found to improve the recovery of the liver from oxidant-mediated damage (Zwacka et al., 1997). In this context, agents that can suppress CD4+ cells infiltration could withhold the subsequent inflammatory cell infiltration, oxidative stress and improve liver tissue histopathological changes.

Amygdalin (Amg., Vitamin B17) is a cyanogenic glycoside compound which belongs to the group widely distributed in plants like apricot and peach (Santos Pimenta et al., 2014; Song and Xu, 2014). Amg. has multiple therapeutic effects as antiatherogenic, antifibrotic, anti-inflammatory and antiulcer agent (Chang et al., 2005; Du et al., 2010; Mirmiranpour et al., 2012). A particular action of Amg. on the liver is the ability to lower levels of AST, ALT, increase hydroxyproline content and inhibit proliferation of connective tissue in CCl4 and D-galactosamine treated rats (Wei et al., 2009).

Exploring the relation between CD4+ cells infiltration and the migration and engraftment of the inflammatory cells with subsequent liver histopathological changes in AIH can help to define new therapeutic agents. The tissue and the cellular distortion accompanying Con A-induced AIH and the postulated protective effect of Amg. were investigated in this study aiming for the implication of nontraditional management procedure.

2. Materials and methods

30 adult male Swiss albino mice (20–22 g) obtained from Mansoura Experimental Research Center, Mansoura, Egypt, were used in this study. The animals were maintained in the animal house, under specific pathogen-free conditions in metal cages with softwood chips for bedding under standard laboratory conditions of temperature and relative humidity. The animals were allowed free access to a standard commercial diet and tap water ad libitum with a 12 h light–dark cycle for two weeks before the experiment for acclimatization and to ensure normal growth and behavior. All the experimental procedures were carried out in accordance with the rules and regulations approved by the Institutional Research Board (IRB) of Mansoura University.

2.1. Chemicals

Concanavalin A (Sigma-Aldrich, St. Louis, MO, USA, product No. C2010) was dissolved in PBS with a concentration of 1 mg/mL. Amygdalin was purchased from Sigma-Aldrich St. Louis, MO, USA (product No. A6005).

Colorimetric kits for alanine aminotransferase (ALT), aspartate aminotransferase (AST), malondialdehyde (MDA), superoxide dismutase (SOD), and reduced glutathione (GSH), were bought from Spectrum Co. (Cairo, Egypt, products of Sigma-Aldrich Nos MAK052, MAK055, MAK085, 19160, and CS0260).

2.2. Animal grouping

The mice were randomly divided into three groups, 10 mice in each group. The control group received a single 15 ml intravenous PBS injection. Con A at a dose of 15 mg/kg body weight was administered by single intravenous injection to induce AIH in the second and the third groups (Fei et al., 2016). AIH-Amg group animals received Amg. 5 mg/kg intraperitoneally once a week for three consecutive weeks (Guo et al., 2013). Seven days after the last Amg. injection, the animals received Con A.

2.3. Sample collection

Twelve hours after the Con A injection, all animals were anesthetized with a mixture of ketamine–xylazine (80 and 10 mg/kg, respectively, i.p.); samples of blood were drawn from the eye sockets and collected in polyethylene tubes after blood centrifugation and kept at −80 C° for further analysis. The livers were rapidly excised and clearly washed with cold normal saline and cut into three parts.

One part of the liver tissue was homogenized, centrifuged for 15 min at 4 C° and the supernatants were kept at –80 C°. The serum levels of ALT and AST were assayed according to the routine biochemical analysis system. The Levels of MDA, SOD, and GSH were determined in hepatic homogenates of different experimental groups based on the methods provided by the kits.

The second part of liver tissue of each animal was fixed in buffered formalin and embedded in paraffin. Specimen (4–5 μm) were placed on polylysine-coated slides and stained with hematoxylin and eosin (H&E), Masson trichrome and CD4 immune stain.

2.4. CD4+ cells immunohistochemistry

Briefly, each paraffin section was deparaffinized and rehydrated through a graded series of ethanol. The antigen retrieval was performed by steaming the slides in the appropriate buffer at different temperatures and pressures. Endogenous peroxidase was blocked using a 3% H_2O_2 methanol solution. 5% bovine serum albumin was applied to block nonspecific staining. Rabbit anti-human CD4 (Sigma-Aldrich, product No. 05-1413) were used for the immunochemistry and counterstained with hematoxylin. Negative control staining was performed with cold PBS, instead of the primary antibody. The detailed steps were in accordance to Niu et al. (2011).

2.5. Electron microscopic examination

For transmission electron microscopy, the third part of the livers was immersed in 5% glutaraldehyde for two hours then washed in 0.1 m phosphate buffer at 4 C° and post-fixed in 1% osmium tetraoxide. After dehydration in gradual series of ethanol, the tissues were embedded in epon 812. Blocks with tissues were cut into semithin sections, then stained with toluidine blue and examined using a light microscope. Representative fields of semithin sections were selected. Ultrathin sections were stained with uranyl acetate and lead citrate, and examined with transmission electron microscope jeol (j.e.m.-100 cxi1) and photographed at 80 k.v. in Mansoura University Electron Microscope Unit.

2.6. Image analysis

The area occupied with fibrous tissue in Masson trichrome stain and CD4+ immune staining was estimated using image analysis estimated by optical density in randomly selected liver samples using (Leica Q Win standard, digital camera CH-9435 DFC 290, Germany). For all measures, ten non-overlapping fields in each paraffin block for each rat were examined at X400 magnification and photographed. The lamp intensity, camera exposure, and camera gain were kept constant throughout the examination. The photographs were analyzed for positive staining using an Image Analyzer with a measuring frame area = 786,432.0 μm2. Morphometry was carried out at the Image Analysis Unit, Anatomy Department, Faculty of Medicine, Taibah University. The relative

Table 1
Effects of Amg. on Con A-induced hepatotoxicity. Serum alanineaminotransferase (ALT), aspartate aminotransferase (AST), liver Malondialdehyde (MDA), Superoxide dismutase (SOD) and Reduced glutathione (GSH). Data are the mean ± SD (n = 10).

	Control group	AIH group	AIH-Amg. group
Serum ALT (U/L)	28.25 ± 1.42	423.45 ± 19.24*** p1 < 0.001	294.14 ± 14.70*** p2 < 0.001
Serum AST (U/L)	43.56 ± 2.76	736.04 ± 36.26*** p1 < 0.001	205.7 ± 14.55*** p2 < 0.001
Liver MDA (nmol/g tissue)	18.62 ± 1.36	54.08 ± 3.59*** p1 < 0.001	22.73 ± 3.12*** p2 < 0.001
Liver SOD (U/g tissue)	17.45 ± 1.82	4.37 ± 0.73*** p1 < 0.001	10.1 ± 1.47*** p2 < 0.001
Liver GSH (umol/g tissue)	13.66 ± 0.76	4.83 ± 0.45*** p1 < 0.001	13.3 ± 0.82*** p2 < 0.001

P1: statistical significance between AIH group versus the control group.
P2: statistical significance between AIH-Amg group versus the AIH group.
p > 0.05 not significant (ns).
*p < 0.05.
**p < 0.01.
*** p < 0.001.

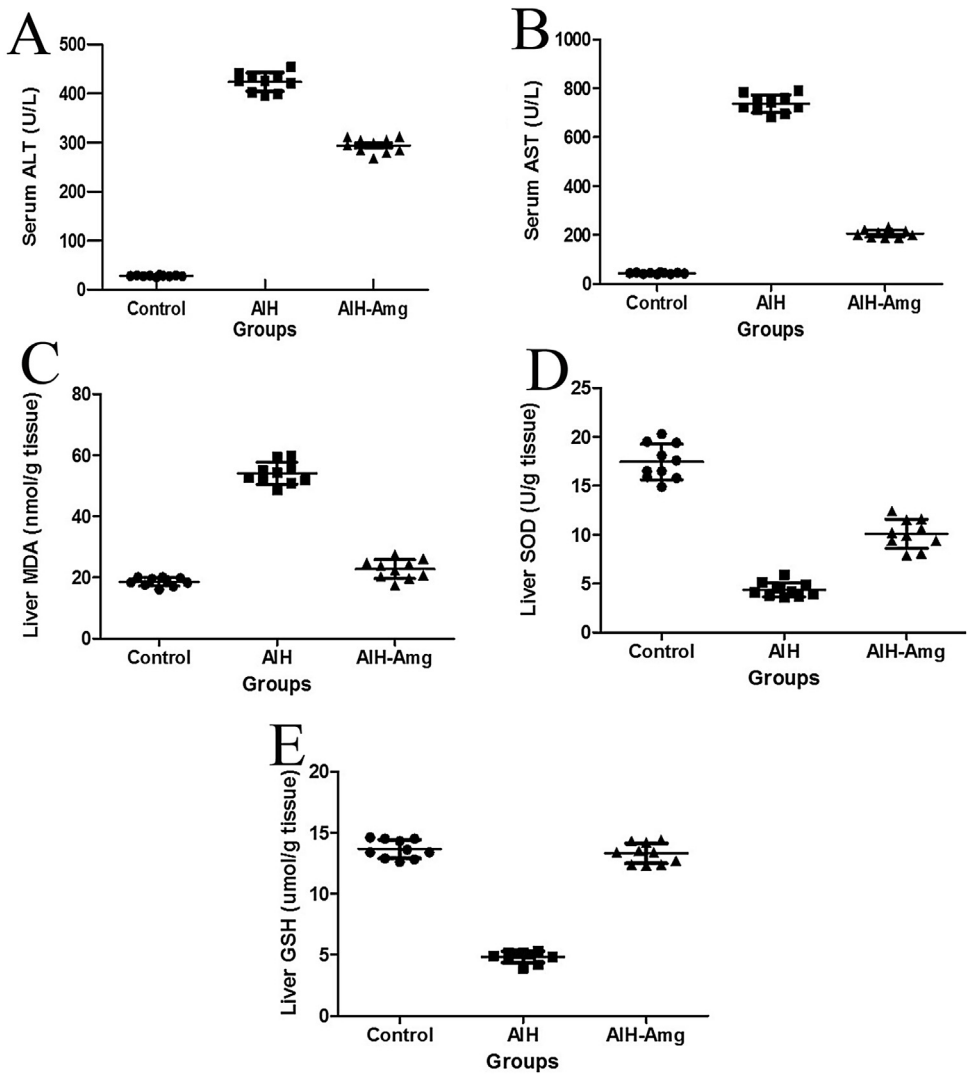

Fig. 1. Amg. pretreatment reverses the increase in the liver enzymes, the liver MDA and decreases SOD and GSH induced by Con A. (A) Serum ALT in the control, AIH and AIH-Amg groups; (B) Serum AST in the control, AIH and AIH-Amg groups; (C) Liver MDA in the control, AIH and AIH-Amg groups; (D) Liver SOD in the control, AIH and AIH-Amg groups; E. Liver GSH in the contol, AIH and AIH-Amg groups.

fibrosis area and CD4+ immune staining were expressed as the percentage of the total liver sectional area.

2.7. Statistical analysis

The data were tabulated, coded and then analyzed using the computer program SPSS (Statistical package for social science) version 24. The results are expressed as mean values ± SD. Normality was verified by the Kolmogorov–Smirnov test. In the statistical comparison between the different groups, the significance of difference was tested using Student's t-test to compare the mean of two groups of numerical (parametric) data. For non- parametric data, Mann-Whitney U- test was used, ANOVA (analysis of variance) was used to compare between more than two groups of numerical (parametric) data and the Kruskal-Wallis for non- parametric data. Significance was accepted at p < 0.05.

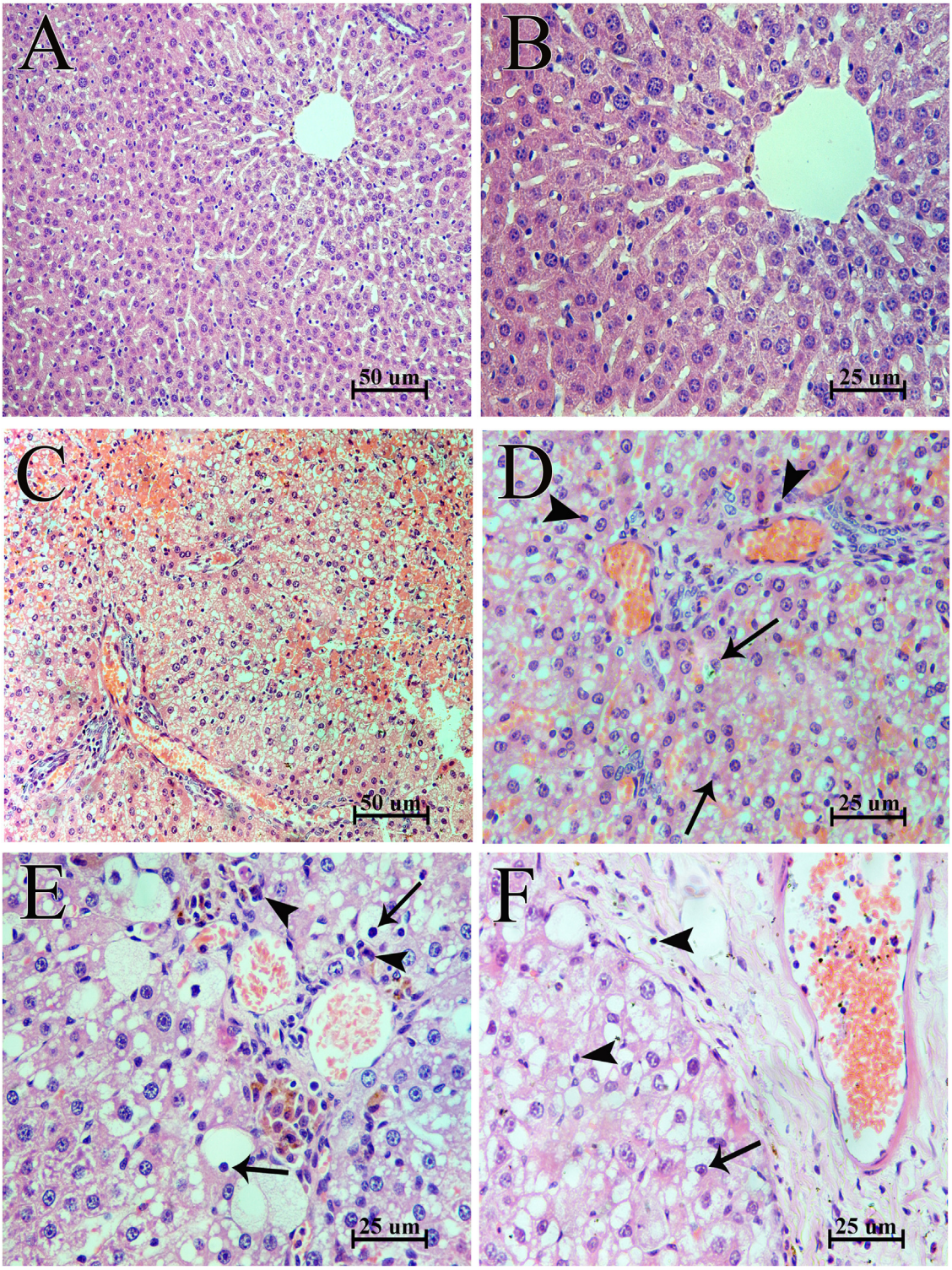

Fig. 2. Histopathological specimens of the liver tissue stained with H&E. (A&B) The control group showing the normal liver architecture with normal central veins and blood sinusoids. (C&D) The AIH group showing extensive interstitial hemorrhage, areas of cloudy swelling and necrosis. The central veins appeared congested and most of the hepatocytes showed signs of degeneration with vacuolated cytoplasm and pyknotic nuclei (arrows). Inflammatory cell infiltration mainly neutrophils can be seen intervening between the hepatocytes (arrowheads). (E&F) AIH-Amg group showed less marked hepatocytes degenerative signs (arrows) and inflammatory cell infiltration (arrowheads).

3. Results

3.1. Biochemical analysis

AIH group showed a significant increase in the serum level of ALT and AST, compared to the control animals. The liver oxidative stress markers showed a significant elevation of MDA and a significant decline in SOD and GSH. Amg. pretreatment in AIH-Amg. group significantly decreased the serum ALT and AST and decreased the liver MDA and SOD and increased GSH to near normal levels compared to the AIH group (Table 1, Fig.1).

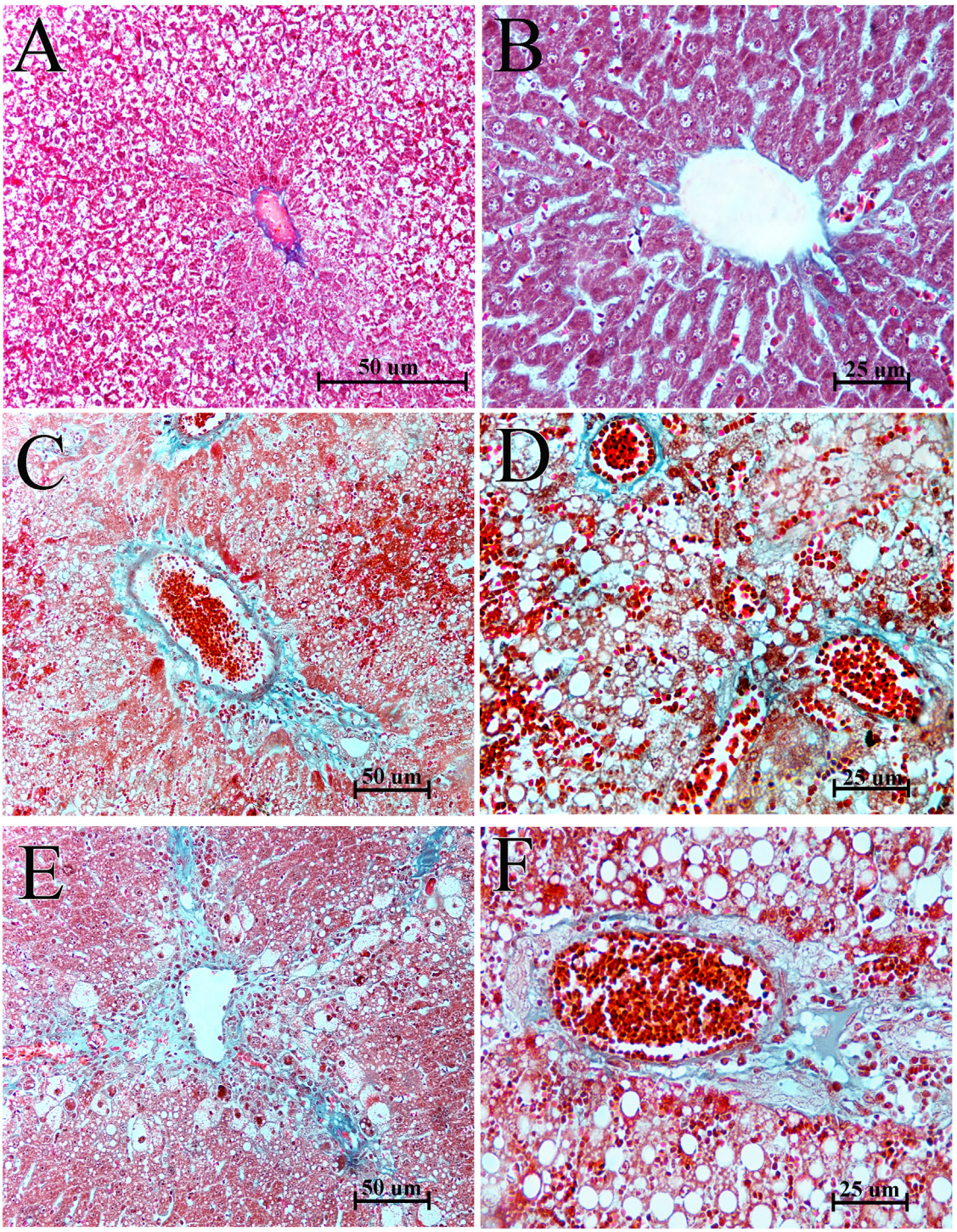

Fig. 3. Masson trichrome stain. (A&B) The control group. (C&D) AIH group, showing blue-stained collagen fibers in the portal tracts and around the central veins. The fibrous septae are seen between distorted liver architecture. (E&F) The AIH-Amg. group had a distorted liver architecture with less marked collagen fibrous septa.

3.2. Histopathological, immunohistochemical studies

In comparison to the controls, H&E stained sections of the AIH group showed distorted hepatic architecture with massive intercellular hemorrhage. The hepatocytes appeared abnormally arranged with areas of extensive necrosis. Most of the hepatocytes showed signs of degenerations with cloudy swelling and apoptotic nuclei separated by congested central veins with inflammatory cell infiltration particularly between the hepatocytes or in the adjacent area to the portal tracts. The AIH-Amg. group showed a less affected tissue degenerative changes and less marked intercellular hemorrhage (Fig. 2).

Masson trichrome stain, in AIH group, showed a relative increase in the amount of the bluish stained collagen fibers in the portal tracts and around the central veins. The fibrous septae could be seen throughout the sections with marked distortion of the liver architecture. The AIH-Amg. group still had a distorted liver architecture with less marked collagen fibrous septa (Fig. 3).

By image analysis, the area percent occupied by collagen fibers were significantly increased in AIH group compared to the control

Table 2
The relative fibrosis area and the CD4+ immuno-staining area expressed as the percentage of the total liver sectional area, in Masson's trichrome-stained and in CD4+ immune stained liver sections. Data are the mean ± SD (n = 10).

	Control group	AIH group	AIH-Amg. group
The relative fibrosis area	0.202 ± 0.02	0.2867 ± 0.07** p1 < 0.01	0.2418 ± 0.03 p2 > 0.05
Relative CD4+ area	11.2117 ± 1.83	29.9316 ± 4.21*** p1 < 0.001	19.6068 ± 4.08*** p2 < 0.001

P1: statistical significance between AIH group versus the control group.
P2: statistical significance between AIH-Amg group versus the AIH group.
p > 0.05 not significant (ns).
*p < 0.05.
** p < 0.01.
*** p < 0.001.

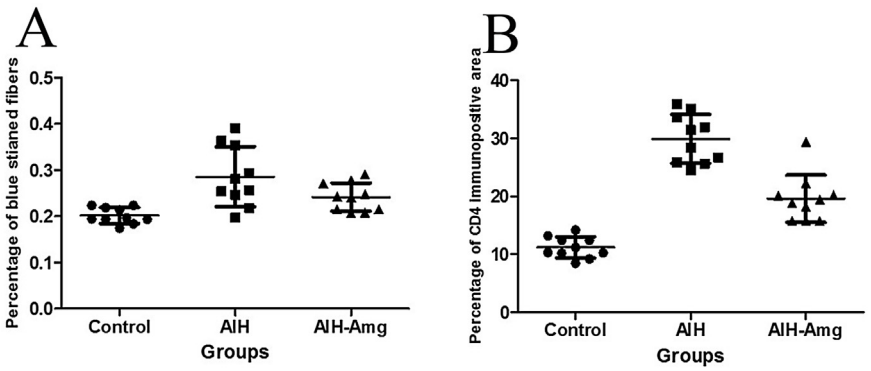

Fig. 4. Amg. pretreatment reverses the increase in the area occupied by collagen fibers and the area of CD4+ immune staining induced by Con A. (A) Area percentage of blue stained fibers in the control, AIH and AIH-Amg groups; (B) Area percentage of CD4+ immune staining in the control, AIH and AIH-Amg groups.

and also non-significantly decreased in AIH-Amg group compared to the AIH group (Table 2, Fig.4).

CD4 immune stained sections of the control group showed positive staining of the endothelium of the sinusoids and negative staining of the endothelium of the central veins. AIH group sections showed a positively stained cytoplasm of cells around the central vein and portal tracts. The immunoreactivity was observed in intervening cells between the hepatic cords (Fig. 5). The AIH-Amg. group showed less marked CD+ cells around the central veins or between the hepatic cords.

The area percent of CD4+ immune staining was statistically increased in AIH group compared to the control. On the other hand, AIH-Amg. group had a significant decrease in CD4 immunoreactivity in comparison to the AIH group (Table 2, Fig.4).

Electron microscopic examination of the control group showed the typical hepatocytes with large rounded euchromatic nuclei and the cytoplasm containing mitochondria, large lipid droplets, and vesicles of the smooth endoplasmic reticulum. The AIH group had a degenerating hepatocyte with irregular shrunken nuclei, irregular swollen mitochondria, disrupted rough endoplasmic reticulum and duplicated nuclear membranes. The AIH-Amg. group showed hepatocytes with variable degrees of nuclear degeneration with less marked cellular changes (Fig.6).

4. Discussion

The immune system plays a major role in the regulation of the liver regenerative and reparative responses. An interaction between the immune cells and liver controls liver regeneration and repair (de et al., 2018). AIH is an immune-mediated inflammatory process triggered by a variety of factors including drugs, alcohol and increased dietary load of free fatty acids (Tsuneyama et al., 2013). AIH can be also propagated by viral infections like hepatitis C, cytomegalovirus, and influenza A viruses (Christen and Hintermann, 2014) through the induction of cytokines and chemokines expression (Christen and Hintermann, 2016).

External inflammatory triggers were used in experimental animals to mimic the features of AIH inhuman. One of the most frequently used ways is the application of Con A. Con A-induced AIH was described as one of the best experimental models for immunological hepatitis (Wang et al., 2012). Con A induces T cell activation and cytokine-mediated severe liver injury in mouse (Tiegs et al., 1992). A single dose of Con A was reported to be sufficient to induce a complete pictured AIH in mice with the availability to investigate the concomitant inflammatory response (Heymann et al., 2015).

The current study showed that Con A injection induced marked hepatic histopathologic injuries with inflammatory cell infiltration and apparently increased tissue fibrosis as manifested by the microscopic examination and confirmed by the high serum levels of ALT, AST and the increase in area percent of fibrosis. The deleterious effects of Con A on the liver were previously reported (Feng et al., 2008; Wang et al., 2019). The cardinal histopathological characteristic of AIH is the patchy piecemeal necrosis affecting the hepatocytes caused by plasmacytosis and red blood cell extravasation (Manns et al., 2015). Different types of inflammatory cells were abundantly present in the portal of AIH sections stretching into the parenchyma (Senaldi et al., 1992).

Although fibrosis is a feature of chronic AIH (Wang et al., 2019; Christen and Hintermann, 2016), as the inflammatory cell infiltrating activates the liver stellate cells (Koyama and Brenner, 2017), the current study showed a significant increase of collagen fibers in AIH group despite the short duration of the experiment. This finding can be explained by the disturbed liver architecture with a relative expansion of the biliary system fibrous tissue. This effect was not marked in AIH-Amg. group as it was eliminated by Amg. pretreatment. Pretreatment with Amg was reported to effective against tissue fibrosis at different durations with the maximum protection at 21 days (Guo et al., 2013).

The present results confirmed the accumulation of oxidative stress marker, MDA contaminant with depressed GSH, SOD in the AIH group. These markers are representative of oxidative stress evoked by reactive oxygen species overproduction (ROS) and asso-

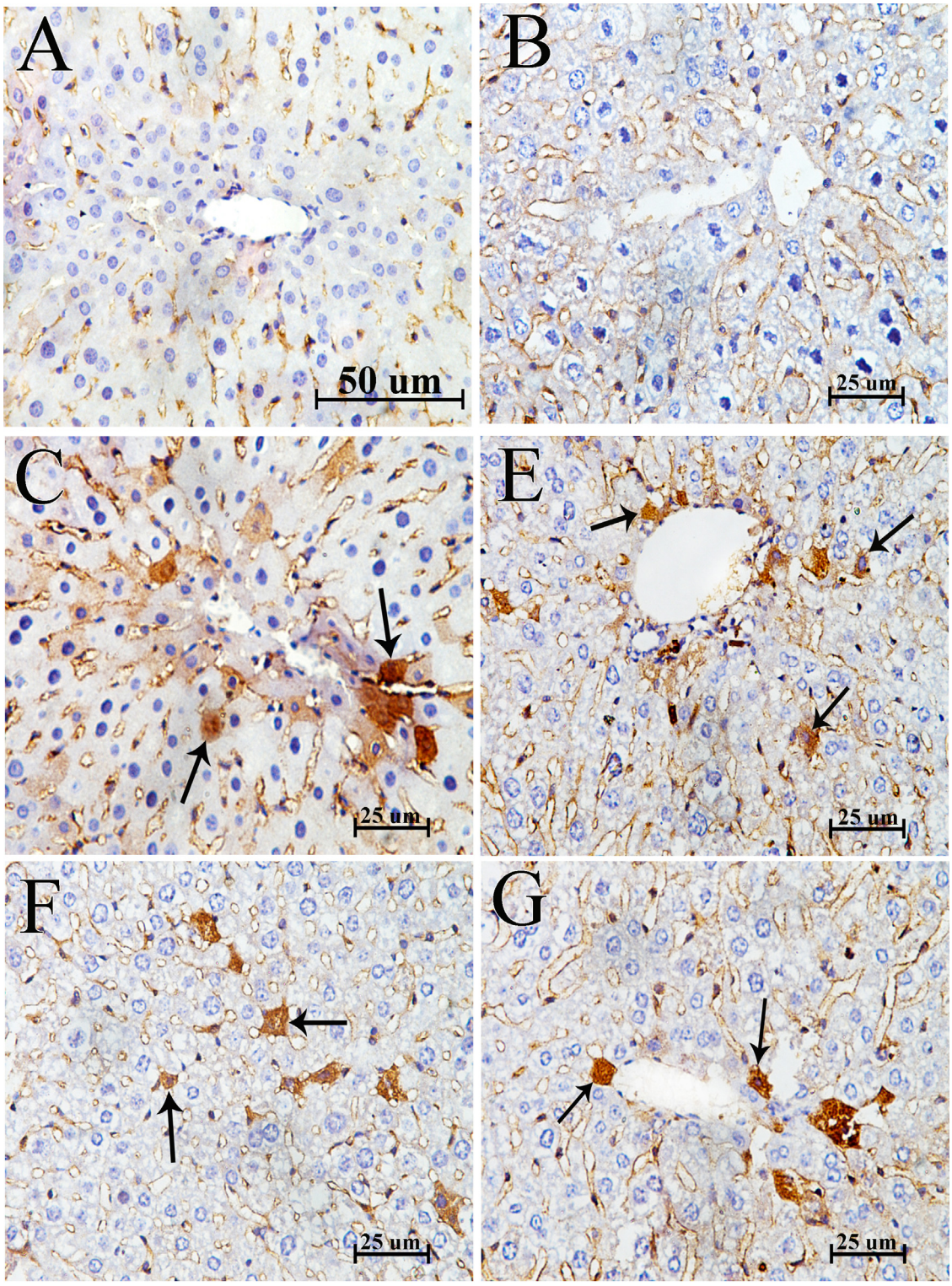

Fig. 5. CD4+ immune staining of the liver section of the control group (A&B) Showing positive staining of the endothelium of the sinusoids and negative staining of the endothelium of the central veins. (C&D) The AIH group showing positively stained cells around the central vein and portal tracts and between the hepatic cords (arrows). (E&G) The AIH-Amg. group showed less made CD+ cells around the central veins or in-between the hepatic cords (arrows).

ciated lipid peroxidation (Nita and Grzybowski, 2016). In Con A-induced hepatitis, the immune inflammatory response induces ROS overproduction which induces increased expression of inflammatory cytokines with subsequent acute inflammation and injury (Wang et al., 2016). The significant decrease in liver MDA and SOD and increased GSH in AIH-Amg is an indicator of decreased ROS production and activation of the antioxidant system mediated by Amg.

A threefold increase in the area percent of CD4+ immune staining was reported only 24 h after AIH induction with increased

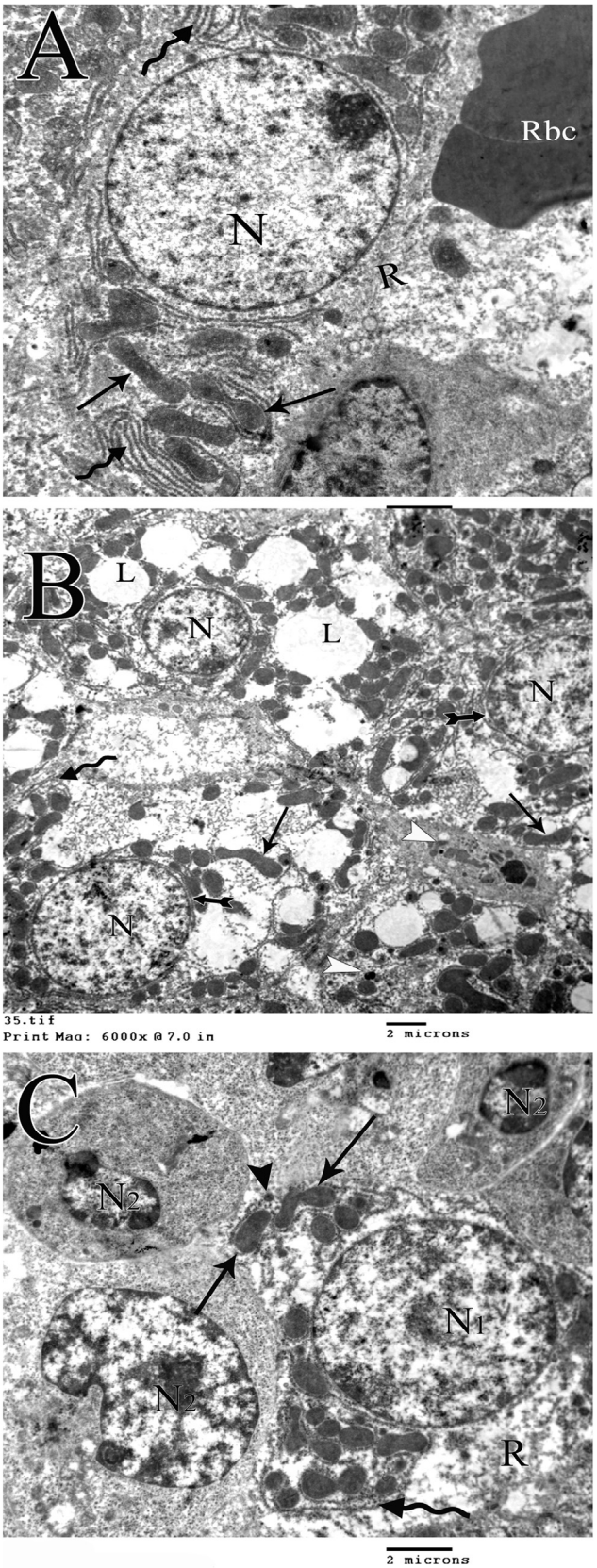

Fig. 6. Electron microscopic examination of the livers of (A) electron micrograph of a control liver (n = 10) showing a part of the liver parenchyma with a hepatocyte facing the liver sinusoids containing red blood cells (Rbc). The cell cytoplasm shows a profile of the rough endoplasmic reticulum (curved arrow), mitochondria (arrows), vesicles of the smooth endoplasmic reticulum (R) and a large euchromatic nucleus (N). (B) the liver parenchyma of Con A-induced AIH (AIH group, n = 10) showing degenerating hepatocytes with shrunken nuclei (N) and multiple lysosomes (white arrowheads). The nuclei showed a double nuclear membrane (tailed arrows). The cytoplasm shows disturbed rough endoplasmic reticulum (curved arrows), bizzar-shaped mitochondria (arrows) and large lipid droplets (L). (C) The parenchyma of AIH-Amg group (n = 10) showing one hepatocyte with a euchromatic nucleus (N1) and three irregular nuclei (N2). The cytoplasm contains mitochondria (arrows), rough endoplasmic reticulum (curved arrow), vesicles of the smooth endoplasmic reticulum (R), few lysosomes (arrowhead).

inflammatory cell infiltration. CD4+ cell infiltration into the liver was reported to occur very early to activate the inflammatory cascade (Zwacka et al., 1997). Con A injection induces CD4+ cells recruitment into the liver where it becomes activated to secrete the cytokines which induce inflammatory reaction (Carambia and Herkel, 2010; Xue et al., 2015).

CD4+ cells control inflammatory cell infiltration and homing in the liver through cytokines production. TNFα and IL-1 facilitate endothelial adherence of neutrophils through either direct activation of neutrophils themselves (Zwacka et al., 1997) or indirectly through changes in surface adhesion molecules on endothelial cells (Yamamoto et al., 2002). A subsequent neutrophil spreading between the damaged liver tissue is mediated by IFNg and GMCSF (Robinson, 2017).

Inflammatory cell infiltrating the liver tissue contribute to liver inflammation (Koyama and Brenner, 2017). The memory phenotype CD4+ cells were reported to be involved in programmed cell death. The accompanied hepatocytes intracellular changes were evidenced in the present study by the electron microscopic examination. The cells showed extensive degenerative changes with irregular shrunken nuclei and abnormal mitochondria and endoplasmic reticulum. These massive changes can be explained by the direct action of the intervened inflammatory cells.

Con A-induced hepatitis was reported to activate T lymphocytes to secrete various cytokines with subsequent increased all liver pathological scores (Ye et al., 2018). Similar ultrastructural signs of cell stress in AIH was reported by Cheng et al. (2014). They inferred these changes to the accompanying inflammatory cascade that activates the autophagy pathway. Another study reported even earlier massive destruction of the hepatocytes was only eight hours after Con A injection (20 mg/kg).

The role of CD4+ cells in controlling liver tissue response to injuries was discussed in many pieces of research. Tiegs et al., (1992) reported complete protection of mice lacking CD4+ cells against Con A-induced hepatitis. An evident decrease in hepatocellular necrosis and evident reduction in neutrophil infiltration in CD4+ cells deficient mice as compared with those with an intact immune system (Zwacka et al., 1997). CD4+ cell infiltration in the hepatic tissue was also linked to other forms of liver injury. CD4+ cell influx to the liver after ischemia was reported within the first hour of reperfusion (Zwacka et al., 1997). On the other hand, CD4+ T lymphocytes depletion have been reported to enhance hepatocellular carcinoma in non-alcoholic fatty liver disease (Ostroumov et al., 2018).

5. Conclusion

The present data demonstrate that Amg. pretreatment protected the liver by reducing the number of infiltrating CD4+ cells. The decreased CD4+ cells infiltration pursued a decreased inflammatory cell infiltration and inhibited AIH-induced tissue and the cellular changes. Amg. protective effect is attributed to its anti-inflammatory and antioxidant activities. These findings suggest that Amg. could be a therapeutic agent in the management of AIH. More detailed studies may be needed for further elucidation of the hepatoprotective effects of Amg.

Funding

This research did not receive any specific grant from funding agencies in the public, commercial, or not-for-profit sectors.

References

Aizawa, Y., Hokari, A., 2017. Autoimmune hepatitis: current challenges and future prospects. Clin. Exp. Gastroenterol. 10, 9–18.

Burak, K.W., Swain, M.G., Santodomingo-Garzon, T., Lee, S.S., Urbanski, S.J., Aspinall, A.I., Coffin, C.S., Myers, R.P., 2013. Rituximab for the treatment of patients with autoimmune hepatitis who are refractory or intolerant to standard therapy. Can. J. Gastroenterol. 27 (5), 273–280.

Carambia, A., Herkel, J., 2010. CD4 T cells in hepatic immune tolerance. J. Autoimmun. 34 (1), 23–28.

Chang, H.K., Yang, H.Y., Lee, T.H., Shin, M.C., Lee, M.H., Shin, M.S., Kim, C.J., Kim, O.J., Hong, S.P., Cho, S., 2005. Armeniacae semen extract suppresses lipopolysaccharide-induced expressions of cyclooxygenase [correction of cycloosygenase]-2 and inducible nitric oxide synthase in mouse BV2 microglial cells. Biol. Pharm. Bull. 28 (3), 449–454.

Cheng, P., Chen, K., Xia, Y., Dai, W., Wang, F., Shen, M., Wang, C., Yang, J., Zhu, R., Zhang, H., Li, J., Zheng, Y., Wang, J., Zhang, Y., Lu, J., Zhou, Y., Guo, C., 2014. Hydrogen sulfide, a potential novel drug, attenuates concanavalin A-induced hepatitis. Drug Des. Devel. Ther. 8, 1277–1286.

Christen, U., Hintermann, E., 2014. Pathogen infection as a possible cause for autoimmune hepatitis. Int. Rev. Immunol. 33 (4), 296–313.

Christen, U., Hintermann, E., 2016. Immunopathogenic mechanisms of autoimmune hepatitis: how much do we know from animal models? Int. J. Mol. Sci. 17 (12).

Czaja, A.J., 2011. Drug-induced autoimmune-like hepatitis. Dig. Dis. Sci. 56 (4), 958–976.

de, H.L., van der Lely, S.J., Warps, A.K., Hofsink, Q., Olthof, P.B., de Keijzer, M.J., Lionarons, D.A., Mendes-Dias, L., Bruinsma, B.G., Uygun, K., Jaeschke, H., Farrell, G.C., Teoh, N., van Golen, R.F., Li, T., Heger, M., 2018. Post-hepatectomy liver regeneration in the context of bile acid homeostasis and the gut-liver signaling axis. J. Clin. Transl. Res. 4 (1), 1–46.

De Biasio, M.B., Periolo, N., Avagnina, A., Garcia de Davila, M.T., Ciocca, M., Goni, J., de, M.E., Galoppo, C., Canero-Velasco, M.C., Fainboim, H., Munoz, A.E., Fainboim, L., Chernavsky, A.C., 2006. Liver infiltrating mononuclear cells in children with type 1 autoimmune hepatitis. J. Clin. Pathol. 59 (4), 417–423.

Du, H.K., Song, F.C., Zhou, X., Li, H., Zhang, J.P., 2010. Effect of amygdalin on serum proteinic biomarker in pulmonary fibrosis of bleomycin-induced rat. Zhonghua Lao Dong Wei Sheng Zhi Ye Bing Za Zhi 28 (4), 260–263.

Ebrahimi, H., Naderian, M., Sohrabpour, A.A., 2016. New concepts on pathogenesis and diagnosis of liver fibrosis; a review article. Middle East J. Dig. Dis. 8 (3), 166–178.

Fei, M., Xie, Q., Zou, Y., He, R., Zhang, Y., Wang, J., Bo, L., Li, J., Deng, X., 2016. Alpha-lipoic acid protects mice against concanavalin A-induced hepatitis by modulating cytokine secretion and reducing reactive oxygen species generation. Int. Immunopharmacol. 35, 53–60.

Feng, D., Mei, Y., Wang, Y., Zhang, B., Wang, C., Xu, L., 2008. Tetrandrine protects mice from concanavalin A-induced hepatitis through inhibiting NF-kappaB activation. Immunol. Lett. 121 (2), 127–133.

Friedman, S.L., 2008. Mechanisms of hepatic fibrogenesis. Gastroenterology 134 (6), 1655–1669.

Gatselis, N.K., Zachou, K., Koukoulis, G.K., Dalekos, G.N., 2015. Autoimmune hepatitis, one disease with many faces: etiopathogenetic, clinico-laboratory and histological characteristics. World J. Gastroenterol. 21 (1), 60–83.

Guo, J., Wu, W., Sheng, M., Yang, S., Tan, J., 2013. Amygdalin inhibits renal fibrosis in chronic kidney disease. Mol. Med. Rep. 7 (5), 1453–1457.

Heymann, F., Hamesch, K., Weiskirchen, R., Tacke, F., 2015. The concanavalin. A model of acute hepatitis in mice. Lab Anim. 49 (1 Suppl), 12–20.

Koyama, Y., Brenner, D.A., 2017. Liver inflammation and fibrosis. J. Clin. Invest. 127 (1), 55–64.

Manns, M.P., Lohse, A.W., Vergani, D., 2015. Autoimmune hepatitis — Update 2015. J. Hepatol. 62 (1 Suppl), S100–S111.

Mao, Y., Wang, J., Yu, F., Cheng, J., Li, H., Guo, C., Fan, X., 2015. Ghrelin reduces liver impairment in a model of concanavalin A-induced acute hepatitis in mice. Drug Des. Devel. Ther. 9, 5385–5396.

Mirmiranpour, H., Khaghani, S., Zandieh, A., Khalilzadeh, O.O., Gerayesh-Nejad, S., Morteza, A., Esteghamati, A., 2012. Amygdalin inhibits angiogenesis in the cultured endothelial cells of diabetic rats. Indian J. Pathol. Microbiol. 55 (2), 211–214.

Nita, M., Grzybowski, A., 2016. The role of the reactive oxygen species and oxidative stress in the pathomechanism of the age-related ocular diseases and other pathologies of the anterior and posterior eye segments in adults. Oxid Med Cell Longev 2016, 3164734.

Niu, Y., Liu, H., Yin, D., Yi, R., Chen, T., Xue, H., Zhang, S., Lin, S., Zhao, Y., 2011. The balance between intrahepatic IL-17(+) T cells and Foxp3(+) regulatory T cells plays an important role in HBV-related end-stage liver disease. BMC Immunol. 12, 47.

Ostroumov, D., Fekete-Drimusz, N., Saborowski, M., Kuhnel, F., Woller, N., 2018. CD4 and CD8 T lymphocyte interplay in controlling tumor growth. Cell. Mol. Life Sci. 75 (4), 689–713.

Robinson, R.T., 2017. T cell production of GM-CSF protects the host during experimental tuberculosis. MBio 8 (6).

Salgame, P., Abrams, J.S., Clayberger, C., Goldstein, H., Convit, J., Modlin, R.L., Bloom, B.R., 1991. Differing lymphokine profiles of functional subsets of human CD4 and CD8 T cell clones. Science 254 (5029), 279–282.

Santos Pimenta, L.P., Schilthuizen, M., Verpoorte, R., Choi, Y.H., 2014. Quantitative analysis of amygdalin and prunasin in Prunus serotina Ehrh. using (1) H NMR spectroscopy. Phytochem. Anal. 25 (2), 122–126.

Senaldi, G., Portmann, B., Mowat, A.P., Mieli-Vergani, G., Vergani, D., 1992. Immunohistochemical features of the portal tract mononuclear cell infiltrate in chronic aggressive hepatitis. Arch. Dis. Child. 67 (12), 1447–1453.

Song, Z., Xu, X., 2014. Advanced research on anti-tumor effects of amygdalin. J. Cancer Res. Ther. 10 (Suppl 1), 3–7.

Tiegs, G., Hentschel, J., Wendel, A., 1992. A T cell-dependent experimental liver injury in mice inducible by concanavalin A. J. Clin. Invest. 90 (1), 196–203.

Tsuneyama, K., Baba, H., Kikuchi, K., Nishida, T., Nomoto, K., Hayashi, S., Miwa, S., Nakajima, T., Nakanishi, Y., Masuda, S., Terada, M., Imura, J., Selmi, C., 2013. Autoimmune features in metabolic liver disease: a single-center experience and review of the literature. Clin. Rev. Allergy Immunol. 45 (1), 143–148.

Wang, H.X., Liu, M., Weng, S.Y., Li, J.J., Xie, C., He, H.L., Guan, W., Yuan, Y.S., Gao, J., 2012. Immune mechanisms of Concanavalin A model of autoimmune hepatitis. World J. Gastroenterol. 18 (2), 119–125.

Wang, K., Song, Z., Wang, H., Li, Q., Cui, Z., Zhang, Y., 2016. Angelica sinensis polysaccharide attenuates concanavalin A-induced liver injury in mice. Int. Immunopharmacol. 31, 140–148.

Wang, Y., Guo, X., Jiao, G., Luo, L., Zhou, L., Zhang, J., Wang, B., 2019. Splenectomy promotes macrophage polarization in a mouse model of concanavalin A- (ConA-) induced liver fibrosis. Biomed Res Int 2019, 5756189.

Wei, Y., Xie, Q., Ito, Y., 2009. Preparative separation of axifolin-3-glucoside, hyperoside and amygdalin from plant extracts by high-speed countercurrent chromatography. J. Liq. Chromatogr. Relat. Technol. 32 (7), 1010–1022.

Xue, J., Chen, F., Wang, J., Wu, S., Zheng, M., Zhu, H., Liu, Y., He, J., Chen, Z., 2015. Emodin protects against concanavalin A-induced hepatitis in mice through inhibiting activation of the p38 MAPK-NF-kappaB signaling pathway. Cell. Physiol. Biochem. 35 (4), 1557–1570.

Yamamoto, S., Sato, Y., Abo, T., Hatakeyama, K., 2002. Morphologic examination of CD3-CD4(bright) cells in rat liver. Wound Repair Regen. 10 (4), 241–244.

Ye, T., Wang, T., Yang, X., Fan, X., Wen, M., Shen, Y., Xi, X., Men, R., Yang, L., 2018. Comparison of concanavalin a-Induced murine autoimmune hepatitis models. Cell. Physiol. Biochem. 46 (3), 1241–1251.

Zwacka, R.M., Zhang, Y., Halldorson, J., Schlossberg, H., Dudus, L., Engelhardt, J.F., 1997. CD4(+) T-lymphocytes mediate ischemia/reperfusion-induced inflammatory responses in mouse liver. J. Clin. Invest. 100 (2), 279–289.